INTERFACE

rsif.royalsocietypublishing.org

Research

Cite this article: Cao F, Zhang C, Choo HY, Sato H. 2016 Insect–computer hybrid legged robot with user-adjustable speed, step length and walking gait. *J. R. Soc. Interface* **13**: 20160060.
http://dx.doi.org/10.1098/rsif.2016.0060

Received: 20 January 2016
Accepted: 3 March 2016

Subject Category:
Life Sciences–Engineering interface

Subject Areas:
biomechanics, biomimetics

Keywords:
insect–computer hybrid robot, legged robot, electrical stimulation, biomechanics, walking gait, biobot

Author for correspondence:
Hirotaka Sato
e-mail: hirosato@ntu.edu.sg

Electronic supplementary material is available at http://dx.doi.org/10.1098/rsif.2016.0060 or via http://rsif.royalsocietypublishing.org.

THE ROYAL SOCIETY PUBLISHING

Insect–computer hybrid legged robot with user-adjustable speed, step length and walking gait

Feng Cao, Chao Zhang, Hao Yu Choo and Hirotaka Sato

School of Mechanical and Aerospace Engineering, Nanyang Technological University, Singapore

HS, 0000-0003-4634-1639

We have constructed an insect–computer hybrid legged robot using a living beetle (*Mecynorrhina torquata*; Coleoptera). The protraction/retraction and levation/depression motions in both forelegs of the beetle were elicited by electrically stimulating eight corresponding leg muscles via eight pairs of implanted electrodes. To perform a defined walking gait (e.g. gallop), different muscles were individually stimulated in a predefined sequence using a microcontroller. Different walking gaits were performed by reordering the applied stimulation signals (i.e. applying different sequences). By varying the duration of the stimulation sequences, we successfully controlled the step frequency and hence the beetle's walking speed. To the best of our knowledge, this paper presents the first demonstration of living insect locomotion control with a user-adjustable walking gait, step length and walking speed.

1. Introduction

Small animals, such as insects, have amazing locomotion and they can swiftly pass through small openings and transverse complex terrains, which has attracted, stimulated and inspired researchers developing many sophisticated miniature robots [1–5], but even the state-of-the-art legged robots cannot compete with living insect locomotion, particularly in terms of controllability, robustness and energy efficiency. As insect physiology has been elucidated to a great extent, researchers have attempted to control insect locomotion by electrically stimulating certain neuromuscular sites to obtain an insect–computer hybrid robot or living insect-based robot, for which a living insect is used as the platform for the robot and the stimulation signals are commanded or output from the user's computer. There are demerits and disadvantages in using an insect platform due to living organisms having a limited lifespan and a relatively narrow operation temperature range. However, here the following major engineering and scientific merits are given.

First, unlike man-made legged robots for which many tiny parts, sensors and actuators are manufactured, assembled and integrated, the insect–computer hybrid robots directly use living insects as Nature's ready-made robot platforms. The only necessary 'assembly' or 'operation' to create an insect–computer hybrid robot is to mount a miniature radio device and implant thin wire electrodes into appropriate neuromuscular sites on the insect for electrical stimulation to induce the desired motor actions and behaviours.

The second advantage of insect–computer hybrid robots over man-made robots is their low power consumption rate (a few milliwatts [6,7]). By comparison, man-made miniature robots of a similar size consume a few hundred milliwatts [8]. Moreover, owing to advanced biofuel cell technology, the insect–computer hybrid robot may be self-powered by energy harvesters embedded in the living insect platform [9–14].

Third, the insect–computer hybrid robot requires neither additional complex structural design nor complicated locomotion control algorithms. In man-made robotics research, the kinematic structure design to realize a robust miniature robot is highly intricate, and the complicated control algorithms for traversing

complex terrain or maintaining posture have posed numerous challenges. However, the insect–computer hybrid robot has developed its own intricate kinematic structure (the motor neuron network and locomotive appendages) through millions of years of natural evolution. Furthermore, the insect maintains its posture in the absence of any control input, negating the need for complicated control algorithms. When the insect–computer hybrid robot encounters an obstacle, the user can simply switch off the controller, allowing the intrinsic neural control networks of the robot to overcome or avoid the obstacle.

Fourth, studies of the electrical stimulation required to induce motor action and behaviour contribute not only to the development of insect–computer hybrid robots, but also to biological science research to explore animal locomotion. Animals exhibit a variety of motor actions and behaviours in their voluntary locomotion (e.g. walking) with a wide dynamic range or limitation in the locomotion parameters including speed, step frequency and step length [15–19]. For example, a cockroach's step frequency is in the range of 3.7–13.5 Hz in its voluntary walking [15]. Investigations into the electrical stimulation required to induce a motor action have suggested that the physical limit of the muscle, for example the maximum force generated by the muscle, can be determined by applying an excessively high-intensity electrical stimulation. In addition, stimulating multiple muscles in a variety of sequences not only mimics the animal's voluntary walking gait but also demonstrates different gaits unseen in natural walking. For example, energetic efficiencies and walking speeds under different walking gaits can be compared to understand whether the voluntary gait is optimal or not. Such investigations would be beneficial for the ecological and evolutionary biology of the insects. Similarly, electrical stimulation studies can reveal the functions and roles of muscles that cannot be determined with certainty by classical anatomical studies. For example, the third axillary muscle, which had previously been thought to have a role solely in wing folding in Coleoptera, has since been shown to have another role in left–right turning in flight through electrical stimulation of the muscle [20]. As such, studies into the electrical stimulation of muscles can help in investigating the physical limit of muscles, in searching for an optimum walking gait by comparing energetic efficiencies and in confirming hypothetical muscle functions.

Within the past two decades, many researchers have been developing animal–computer hybrid robots [6,7,20–45]. Platforms of animal–computer hybrid robots include beetles (*Mecynorrhina torquata*) [6,7,20], hawkmoths (*Agrius convolvuli* and *Manduca sexta*) [22–27], cockroaches (*Periplaneta Americana* and *Gromphadorhina portentosa*) [29,31,41–45] and spiders (*Heteropoda venatoria*) [46]. In these studies, control was administered by neuromuscular stimulation. In the walking control of cockroaches, researchers incited turning motions by tactile, thermal or electrical stimulation of the antennae. Right and left turning by spiders was controlled by neural stimulation of a ganglion. Although the cockroach and spider studies demonstrated successful control of the walking direction, they did not attempt to control the walking speed and gait. Walking control with such user-adjustable modes and parameters would improve the agility of the insect–computer hybrid robot towards practical applications.

In this study, to understand the sequence of leg motions in an insect's voluntary walking gait, the detailed leg motions were tracked by a three-dimensional motion-capturing system and analysed to obtain the time sequence of each motion. Then, custom-programmed sequences for leg muscle stimulation to generate different walking gaits and to operate the sequences using a microcontroller were developed. Next, the resultant step length and walking speed as a function of the insect–computer hybrid robot's step frequency were obtained and discussed. Lastly, a repeatability test was carried out on four beetles to obtain the standard deviation of the elicited leg's angular displacement. Although the ultimate goal of this research is to control all six legs of an insect, because our earlier studies enabled us to elicit the desired motor actions in the front legs of beetle, initially this study has targeted the front legs alone to control their motions to achieve two-leg-based walking gaits with adjustable speed and step frequency.

2. Material and methods

2.1. Study animal

Adult *M. torquata* (order Coleoptera, about two months old, purchased from Kingdom of Beetle Taiwan) were used as the insect platform for the insect–computer hybrid robot. The beetles were reared in plastic vivaria of dimensions 15 cm (length) × 15 cm (width) × 20 cm (height) and fed with sugar jelly every 2–3 days. Each beetle was reared in a single plastic vivarium at constant temperature (approx. 25°C) and relative humidity (approx. 60%). Only male beetles 6–8 cm long and weighing around 7 g were used in the experiments.

2.2. Insect anatomy

The muscles controlling the leg motions were located in an anatomical study of the beetle's front leg. Prior to the anatomical study, the beetle was immersed in 95% ethanol solution (Aik Moh Paints & Chemicals Pte Ltd, Lot 1409T029) for approximately 12 h. The beetle's cuticle was cut open with micro-dissecting spring scissors (Vannas® straight scissors with 3 mm cutting edge, 0.15 mm tip width). The cuticle was then removed with tweezers (Dumont® tweezer, pattern no. 5, tip size 0.05 × 0.01 mm) to expose the muscles. The front leg muscles stimulated in the walking control are shown in figure 1. The protraction and retraction muscles inside the beetle's prothorax control the protraction and retraction motions of the front leg (by which the leg swings forwards and backwards about the thorax–coxa joint; see figure 1*a*). The levation and depression muscles inside the coxa enable levation and depression motions of the femur (which rotates about the coxa–trochanter joint; see figure 1*b*). The retraction and depression muscles are larger than the corresponding protraction and levation muscles, because retraction and depression are performed when the leg touches the ground; thus, they execute the power stroke that pushes the body forwards. The protraction and levation muscles are used when the leg is in the air, performing the return stroke that brings the leg forwards. The power stroke requires more main forces than the return stroke.

2.3. Implantation of stimulation electrodes

A pair of stimulation electrodes was implanted into each muscle. The beetle was fixed onto a wooden block by wrapping softened dental wax (Cavex Set Up Modeling Wax immersed in 80°C water for 10 s) around its body. Holes of 0.5 mm diameter were made on the beetle's cuticle using an insect pin (Indigo Instruments, no. 3 black enamel insect pin) at the sites indicated by red crosses in figure 1. The stimulation electrodes were thin silver wires (A-M Systems, diameter = 127 µm without insulation; 178 µm with Teflon insulation coating). The insulation at the end of the silver wire was removed by flame-heating. To ensure the correct implantation depth, a metal stopper knot was soldered approximately 2 mm from the tip of the stimulation electrode.

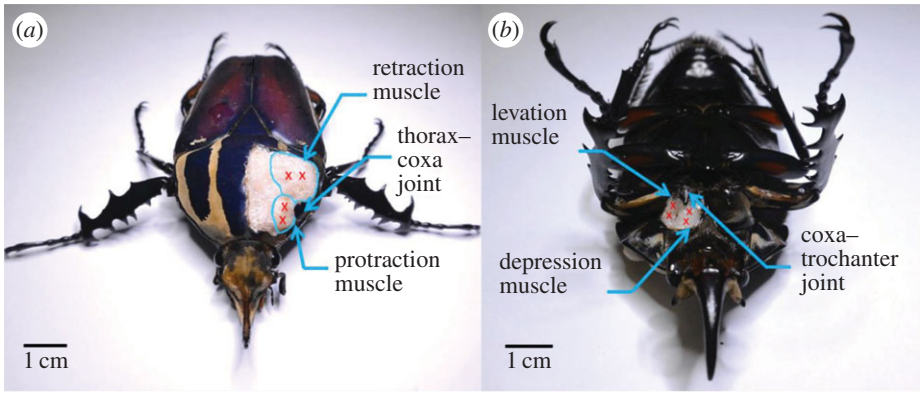

Figure 1. Insect platform for the legged robot and its front leg anatomy. (*a*) Beetle's front leg anatomy. The protraction and retraction muscles (inside the prothorax) enable the leg to swing forwards and backwards about the thorax–coxa joint. (*b*) The levation and depression muscles (inside the coxa) enable levation and depression motions of the femur about the coxa–trochanter joint. Red crosses mark the sites of stimulation electrodes implanted into each muscle.

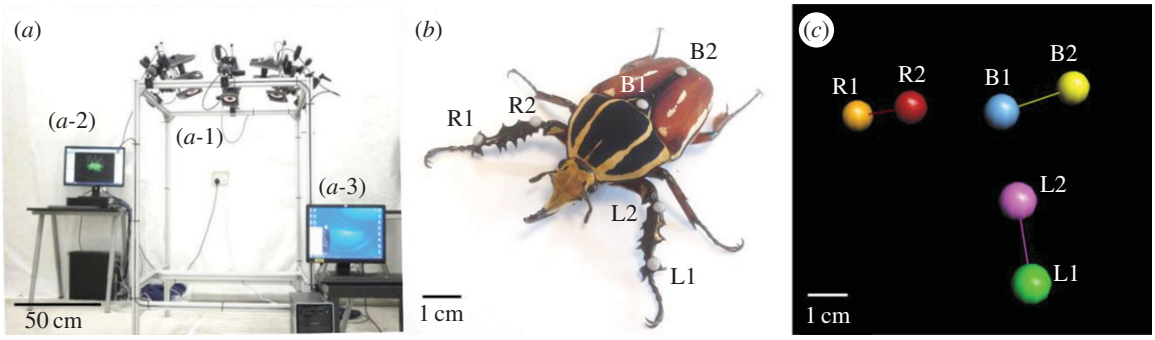

Figure 2. Experimental set-up for the walking gait investigation. (*a*) Three-dimensional motion-capturing system used for recording and storing the three-dimensional position information of the markers attached on the beetle. (*a*-1) Six T40 s VICON® cameras of 4 megapixels (2336 × 1728) resolution operating at 100 fps for motion recording. (*a*-2) The VICON® server was used to reconstruct, store and export the marker position information collected by the cameras. (*a*-3) The computer was custom-programmed in MATLAB® for the walking gait analysis. (*b*) Two reflective markers were attached to each of the beetle's front legs (L1, L2, R1 and R2), representing the tibia segments. Two additional reflective markers (B1 and B2) were attached to the beetle's body, allowing tracking of the walking direction and body orientation. (*c*) The collected three-dimensional motion data of both tibia segments and the body segment were displayed as three independent segments. To represent the tibia sections of the right and left legs and the beetle's body, we linked markers R1 and R2, L1 and L2, and B1 and B2, respectively.

The other end of the stimulation electrode was connected to the output of the stimulation signal-generating circuit.

2.4. Walking gait study

We used a three-dimensional motion-capturing system (figure 2*a*) to record the Cartesian coordinates of the beetle's front tibia sections with time stamps during voluntary straight line walking. The three-dimensional motion-capturing system consists of six T40 s VICON® cameras, each with resolution of 4 megapixels (2336 × 1728) operating at 100 frames per second (fps) (figure 2*a*1). As shown in figure 2*b*, each of the beetle's front tibia segments was attached with two reflective markers (L1, L2, R1 and R2; MoCap Solutions, 3 mm hemispherical marker) for motion-capturing purposes. For tracking the beetle's walking direction and body orientation, two reflective markers (B1 and B2; MoCap Solutions, 3 mm hemispherical marker) were attached to the beetle's body. The experimental arena was a horizontal surface of approximately 1 m^2. The global reference frame of the three-dimensional motion-capturing system was set so that its *x*- and *y*-axes formed the horizontal plane parallel to the beetle's walking surface. The *z*-axis was thus perpendicular to the walking surface. The collected three-dimensional motion data were displayed as three independent segments, representing the tibia segments of the two front legs and the body segment (figure 2*c*). The motion data were then exported as comma-separated value (CSV) files and analysed by custom-programmed MATLAB® codes. The walking gaits of five beetles were recorded and analysed.

2.5. Sequential electrical stimulation signals for walking control

Waves with pulse-width modulation (PWM) were applied to different muscles at predefined timings to elicit the desired leg motions for walking control. The PWM stimulation signal was produced by a custom-programmed microcontroller (Texas Instruments, CC2530, 6 × 6 mm^2, 32 MHz clock) and a customized external circuit. Using the timer interrupt function embedded in the CC2530 microcontroller, we programmed the pulse width and frequency of the stimulation signal to be user adjustable. Figure 3*a* shows the CC2530 microcontroller connected to the external circuit for stimulating one muscle. An input/output (I/O) pin and the ground (GND) pin formed one channel to generate PWM waves. To stimulate each muscle, one input of an optocoupler (ISOCOM Components, ISP817X) was connected to one of the I/O pins (set to output mode); the other was connected to the GND pin of the microcontroller. Both outputs of the optocoupler were connected in series with a 1.5 V battery (Sony Corporation, dry battery, AA R6 SUM3) and the target muscle. For fast release of the residual charge in the optocoupler, a 470 Ω resistor (Multicomp, wirewound, 3 W) was connected in parallel with the muscle to be stimulated. In this configuration, the optocoupler functioned as a switch in the muscle stimulation circuit (figure 3*a*). The I/O pins of the CC2530 microcontroller were used as the on–off controls of the optocoupler and to power the light-emitting diode (LED) in the external circuit as an indicator of muscle stimulation status. The PWM waves with 1 ms pulse

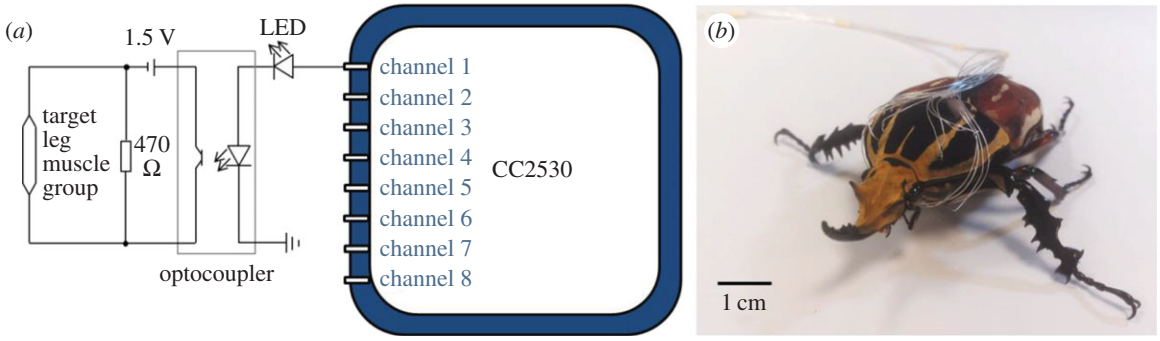

Figure 3. Circuit diagram of the insect–computer hybrid robot. (*a*) The CC2530 microcontroller connected to the external circuit for stimulation of one muscle. The PWM wave generation was controlled via the I/O pins (channels 1–8) and the GND pin of the microcontroller. The circuit consists of an LED (for stimulation status indication), an optocoupler (acting as a switch for the muscle stimulation circuit), a 470 Ω resistor (for fast release of the residual charge in the optocoupler) and a 1.5 V battery (for power supply for muscle stimulation). Channels 1–8 separately controlled the eight identical external circuits that stimulated the eight muscles in the beetle's two front legs. (*b*) A beetle with 16 stimulation electrodes (two electrodes per muscle) implanted into the eight muscles (controlling protraction, retraction, levation and depression motions in both front legs). Channels 1–8 generated stimulation signals in a predefined sequence for the walking control of the beetle.

width and 1.5 V amplitude are set to elicit muscle contraction (and the corresponding leg motion) [6]. The main function of the microcontroller code for the walking control is shown in the electronic supplementary material, code S1; additional information on the code is available upon request.

The protraction/retraction muscles (by which the leg swings forwards and backwards in the frontal plane) and the levation/depression muscles (by which the leg lifts from and lowers onto the walking surface) of the front legs were stimulated sequentially for walking control. Therefore, eight stimulation channels were used to separately control the four motion types of the two front legs, and all other leg motions were restricted by inserting insect pins at the leg joints. The coxa of the middle leg was restricted at its maximum retraction angle to avoid blocking the front leg when the front leg performed retraction. Figure 3*b* shows the implanted insect–computer hybrid robot. Various alternating tripod walking gaits are adopted by around 3 million species of insects [47], and very recently a galloping walking gait was discovered in the species of flightless desert dung beetles (*Pachysoma*) [48]. In the tripod walking gait of a six-legged insect, one leg always moves out of phase with its contralateral pair (i.e. the middle leg on one side moves synchronously with the contralateral front leg and hind leg). On the other hand, in a galloping walking gait, the legs of a pair always move synchronously (in-phase). As only the two front legs were electrically stimulated and involved in the walking gait while the middle and hind legs were constrained (pined), the walking gaits demonstrated are technically neither tripod nor galloping. For convenience, we named the two walking gaits of our insect–machine hybrid robot as tripod and galloping. In real life, a six-legged insect was also observed to move exclusively with two legs. The cockroach (*Periplaneta americana*) was recorded propelling itself only with two hind legs by increasing its body's angle of attack during fast running (running speed above 1 m s^{-1}) [17]. For our insect–computer hybrid robot, as we can control the individual motions of each leg, the locomotion gait can be more user-adjustable than the case when some sensory pathway (e.g. antenna, ganglion) is stimulated, in which the induced locomotion control is based on the insect's natural walking.

2.6. Investigating the effect of step frequency on the walking speed and step length in the tripod and galloping walking gaits

As both the walking gait and step frequency of the insect–computer hybrid robot are user adjustable, we experimentally investigated the effect of step frequency on the beetles' walking speed and step length in both gaits (tripod and galloping). The walking control experiment was conducted on an exterior polystyrene foam arena with dimensions of 120 cm (length) × 60 cm (width) × 5 cm (height). A camera (Panasonic® HC-X920M, 20.4 megapixels, 25 fps) was fixed above the beetle and perpendicular to the horizontal walking surface. For calibration purposes, a 30 cm ruler was placed parallel to the beetle's walking path. Six beetles were filmed during tripod and galloping walking at different step frequencies (2, 1, 0.5, 0.25 and 0.125 Hz). The beetles were tested on the same day as they were implanted. The walking speed study yielded 90 data points (nine for each step frequency in each walking gait). Moreover, at each step frequency and walking gait, the average walking speed was calculated from five continuous steps (excluding the first and last steps), providing 150 data points for the step length analysis (75 each from the left and right legs). The walking control films were manually extracted frame by frame using the Avidemux 2.6® video editor. The extracted pictures were then opened in Microsoft® Paint and manually analysed pixel by pixel. As shown in figure 4, the step length was obtained by measuring the distance between consecutive anterior extreme positions (AEPs) of the front leg [49]. The pixel coordinates at the articulation connecting the tibia and tarsus indicate the leg's contact point with the ground (red crosses on the left leg in figure 4). The instant at which the leg reached its AEP was determined from the LEDs, indicating the signal output of the stimulated walking control (at the AEP, the protraction and depression muscles were simultaneously stimulated just before the stimulation switched from the protraction to retraction muscles; the details are presented in table 1).

2.7. Repeatability study of leg motion elicitation

To test the repeatability of electrically induced leg motion, the protraction/retraction muscles of the front leg were alternatively stimulated for 1 s to elicit the cycle of protraction and retraction motions of the fore leg: the channel for the protraction muscle stimulation was turned on for 1 s, then that channel was turned off and another channel for retraction muscle stimulation was turned on for 1 s (thus, the frequency was 0.5 Hz). The cycle was repeated for at least 30 min per day for 7 consecutive days. The leg's motions were tracked and recorded using the same technique as described in §2.4. Two-factor analysis of variance (ANOVA) was conducted at the 95% confidence level to quantitatively evaluate the significance of the effects of the beetle and test day on the mean and standard deviation of the leg's angular displacement. All statistical analyses were performed using Microsoft® Excel 2010.

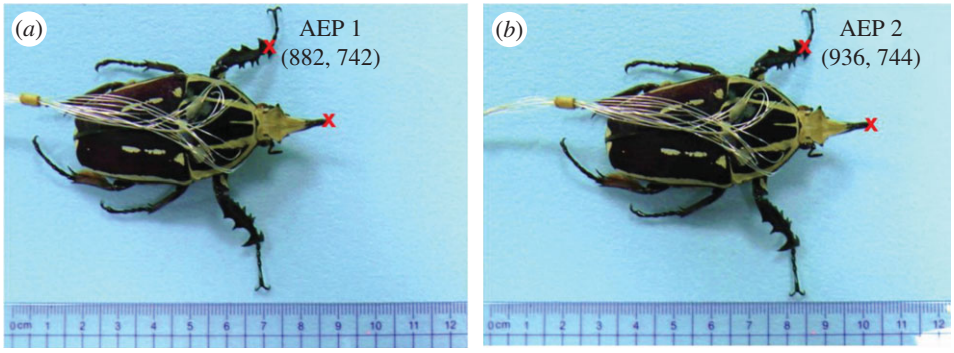

Figure 4. Experimental set-up of the walking speed versus step frequency analysis. (*a*) Snapshot of the insect–computer hybrid robot during galloping with both front legs at their first AEPs. (*b*) One step later, with both front legs at their second AEPs. Red crosses indicate the pixel coordinates of the articulation connecting the beetle's left tibia and tarsus, used to calculate the step length. The beetle's walking distance was determined from the distance travelled by the beetle's horn (indicated by the red cross on the horn). The pixel distance between AEP 1 and AEP 2 was calculated by Pythagoras' theorem. The pixel distance was then converted to the actual distance (in centimetres) travelled by the leg by calibration with a 30 cm ruler.

Table 1. Stimulation sequences of the beetles' walking control in tripod and galloping gaits. Filled and open dots indicate that the stimulation channel was switched on and off during the motion, respectively.

	right leg				left leg			
	protraction	retraction	levation	depression	protraction	retraction	levation	depression
stimulation sequence for tripod walking gait								
1	●	○	●	○	○	●	○	●
2	●	○	○	●	○	●	●	○
3	○	●	○	●	●	○	●	○
4	○	●	●	○	●	○	○	●
stimulation sequence for galloping walking gait								
1	●	○	●	○	●	○	●	○
2	●	○	○	●	●	○	○	●
3	○	●	○	●	○	●	○	●
4	○	●	●	○	○	●	●	○

3. Results and discussion

3.1. Walking gait study

To study the front leg motion of the beetle, we constructed a stick diagram of the tibia segment at different times (figure 5) [49]. Here, we used the motion data of free movement in a straight line. Figure 5 illustrates the lateral view of the motion trajectory of the front tibia segment. As the camera frame rate of motion capture was set to 100 Hz, any two consecutive sticks are 10 ms apart. The horizontal axis indicates the distance travelled by the tibia segment along the beetle's walking direction. For example, if the beetle travelled along the x-axis of the global reference frame (i.e. the y-coordinates of the two markers on its body remained constant), the horizontal axis of figure 5 would coincide with the x-axis of the global reference frame. The vertical axis of figure 5 indicates the vertical distance travelled by the front tibia segment (which coincides with the z-axis of the global reference frame). The blue and red sticks in figure 5 represent the anterior extreme positions (AEPs) and posterior extreme positions (PEPs), respectively, of the beetle's front leg. When the motion progresses from a blue stick to a consecutive red stick, the leg is performing a power stroke (a retraction that swings the leg backwards relative to the body). Conversely, when the motion progresses from a red stick to a consecutive blue stick, the leg is performing a return stroke (a protraction that swings the leg forwards relative to the body). Moreover, an increase or a decrease of the marker's vertical position indicates that the leg is being levated or depressed, respectively.

During voluntary walking, the power and return strokes were repeated. The four motion types (protraction, retraction, levation and depression) were performed with different timings, generating cyclic leg motions. The duration of each motion type was extracted from figure 5 by counting the number of sticks involved in that motion (as mentioned above, the time interval between two consecutive sticks was 10 ms). A complete walking step is defined as the duration between two consecutive AEPs [49]. Figure 6 shows the duration of the four motion types of the front leg, normalized by the corresponding step period (number of beetles = 5, number of steps = 25). The average duration of a complete walking step was 900 ± 600 ms (mean $\pm$ s.d., corresponding to a step frequency of 1.66 ± 0.93 Hz). Retraction and depression were executed concurrently in the power stroke and occupied the first $61 \pm 22\%$ of a complete walking step (red and green bars in figure 6). The return stroke comprised

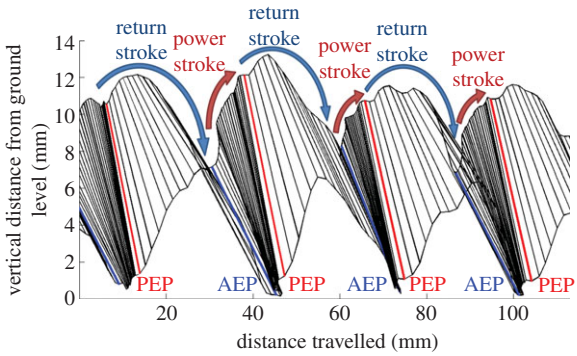

Figure 5. Stick diagram for walking gait analysis of an intact beetle. Lateral view of the motion trajectory of the tibia segment of the beetle's front leg. The time between two consecutive sticks was 10 ms. The horizontal and vertical axes indicate the forward and upward distances travelled by the tibia segment, respectively. The progression from one blue stick (AEP) to the next blue stick (the consecutive AEP) indicates a walking step. Levation (depression) motions are indicated by an increase (decrease) in the marker's vertical position.

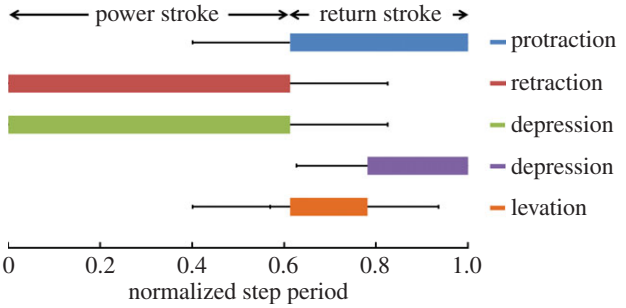

Figure 6. Time intervals of the four motions, normalized by the corresponding step duration ($N = 5$ beetles, $n = 25$ steps). The four motion types (protraction, retraction, levation and depression) were performed at different timings to generate the cyclic power and return strokes during voluntary walking. First, retraction and depression (red and green bars, respectively) were executed concurrently during the power stroke (comprising the first $61 \pm 22\%$ of a complete walking step). During the following return stroke, protraction (blue bar) was executed throughout, whereas levation (orange bar) was switched to depression (purple bar) at $78 \pm 15\%$ of the normalized step duration.

protraction, levation and depression. Protraction was executed throughout the return stroke, whereas levation was converted to depression at $78 \pm 15\%$ of the normalized step duration. Similar leg motion sequences have been observed in the firing sequence of the motor neurons during middle leg motions of a voluntary walking stick insect [50]. In that study, the motor neuron pools controlling the retraction and depression were activated during the power stroke, whereas the motor neuron pools controlling the protraction (levation and depression) were activated during the return stroke (in the early and late phases, respectively) [50]. The step length was normalized by the beetle's body length. The average step length of voluntary walking was 0.24 ± 0.08 body length (mean $\pm$ standard deviation, number of beetles $= 5$, number of steps $= 25$).

3.2. Leg motion and walking gait control

A full walking step of a legged robot involves a power stroke and a return stroke [51]. From the walking gait study, we represented the durations of the four leg motion types as proportions of the entire duration of a walking step (figure 6). In the actual walking control of the beetle, we imposed protraction and levation only during the return stroke and equalized the durations of the return and power strokes. These specifications simplified the leg motions and therefore the walking analysis (step frequency and step length analysis). As such, in the actual walking control, the power stroke starts from the AEP when the leg performs both retraction (for the backward swing) and depression (for the ground contact), generating the forward propulsion for the body. At the end of the power stroke, the leg is brought to the PEP and the depression switches to levation. During the succeeding return stroke, the leg performs both protraction (for the forward swing) and levation (lifting the leg from the ground). At the end of the return stroke, the leg is brought back to the AEP and the levation switches to depression. The resulting leg motion control consists of cyclic repetitions of these power and return strokes. The leg muscle stimulation sequence is shown in table 1. In both gaits (tripod and galloping), stimulation sequence 1 of the right leg control consists of protraction and levation for the return stroke. The leg is then switched from the return stroke to the power stroke by activating protraction and depression in stimulation sequence 2. Stimulation sequence 3 consists of retraction and depression for the power stroke. Finally, the power stroke is switched to the return stroke in stimulation sequence 4, which simultaneously elicits retraction and levation. Stimulation sequences 1–4 were repeated in both gaits to generate cyclic power and return strokes. However, in the tripod walking control, the muscles stimulated in the left leg were always antagonistic to those stimulated in the right leg. In the galloping control, the muscles of both front legs were stimulated in the same stimulation sequence, so that both legs always performed the same motions at the same time. Figure 7*a*,*b* illustrates the elicited leg motions during the stimulation sequences of tripod and galloping control (table 1), respectively. Figure 7 shows the ventral view of the beetle for clear demonstration of the leg motion control. Compared with antenna stimulation in the cockroach [29,41–45] and ganglion stimulation in the cockroach and spider [31,46], appendage muscle stimulation enabled user-adjustable walking gait and step frequency control. However, whereas just two pairs of electrodes were used for the antenna or ganglion stimulation, eight pairs of electrodes are necessary for the two-leg-based walking control of this study. In order to perform the entire six-leg-based walking control in reality, reducing the number of stimulation electrodes would reduce the tediousness of implantation, for example by setting a counter (GND) electrode to be commonly used for all the working (I/O) electrodes would reduce the number of implanted stimulation electrodes by half.

3.3. Walking speed and step length analysis

Besides controlling the walking gait, we aimed to control the step frequency and thereby the walking speed of the beetle. The step frequency was controlled by altering the durations of the stimulation sequences in table 1 and investigating the resultant walking speeds of the insect–computer hybrid robot. In both tripod and galloping gaits, we set the stimulation durations of each sequence to 0.125, 0.25, 0.5, 1 or 2 s, corresponding to step frequencies of 2, 1, 0.5, 0.25 and 0.125 Hz,

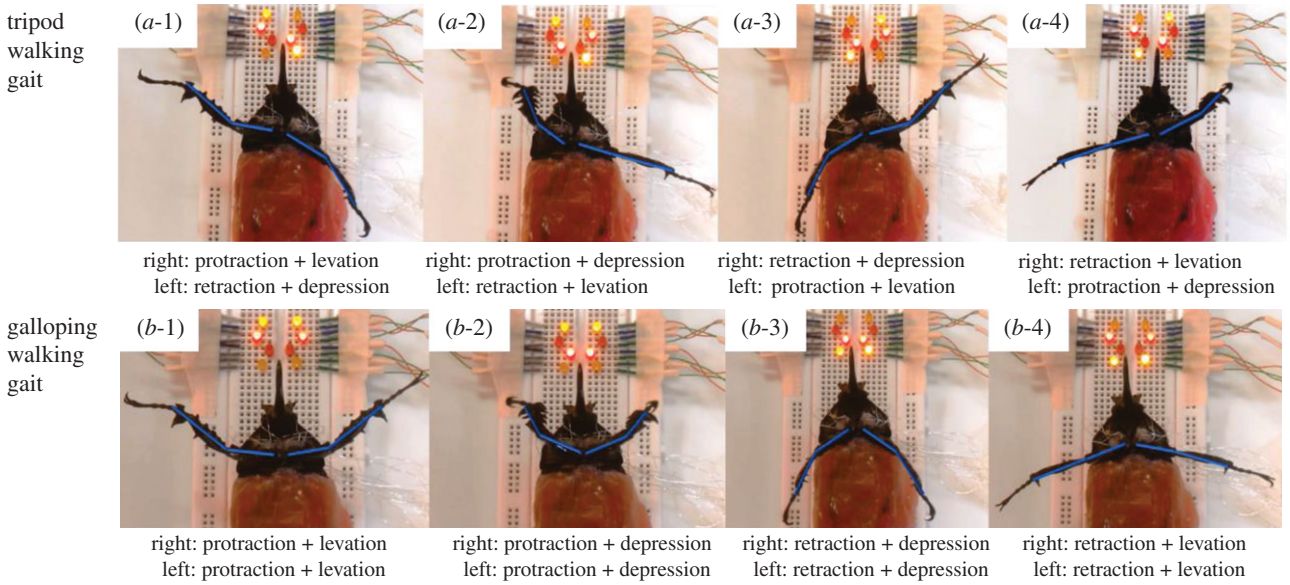

Figure 7. Demonstration of sequential leg motion control in tripod and galloping gaits. Videos were shot from the beetle's ventral view for clear viewing of the resultant leg motions during the predefined stimulation sequence (table 1). (*a*-1)–(*a*-4) and (*b*-1)–(*b*-4) are the leg motions under stimulation sequences 1–4 during tripod and galloping walking control, respectively. LED lights near the beetle's head indicate the on–off status of the corresponding stimulation channel.

respectively (recall that sequences 1–4 constitute a single walking step). Figure 8 plots the relationship between the normalized walking speed (body lengths per second) and the step frequency of six beetles. Each walking speed was averaged from five continuous steps (excluding the first and last steps). As evident in the figure, the average normalized walking speed was always higher in the galloping gait than in the tripod gait, for all the step frequencies tested. This is because in the tripod gait, where the two front legs move out of phase, the leg performing the power stroke not only propels the body forwards but also turns the body in the contralateral direction. In the galloping gait, the two front legs move synchronously, pushing the body straight ahead during the power stroke. Therefore, at a given step frequency, the average step length (normalized by the body length of the corresponding beetle) was larger during galloping than during tripod walking (figure 9). As such, the galloping gait propelled the body more efficiently than the tripod gait, and the insect–computer hybrid robot walked faster in the galloping gait than in the tripod gait at the same step frequency.

In both gaits, the average normalized walking speed of the robot increased with increasing step frequency up to 1 Hz, and then decreased after further doubling the step frequency to 2 Hz (figure 8). The walking speed was maximized at 0.26 body lengths per second (2.00 cm s^{-1}) in the galloping gait at a step frequency of 1 Hz. In walking speed studies of a man-made robot [52] and a voluntary walking animal [15], the walking speed was observed to be directly proportional to the step frequency. In other words, for a constant step length, the walking speed would double with each doubling of the step frequency. However, in this study, the normalized walking speed was a nonlinear function of the step frequency (despite being an increasing function of the step frequency up to 1 Hz). For instance, when the step frequency was doubled from 0.125 to 0.250 Hz, the average normalized walking speed increased by 77% in both tripod and galloping gaits. Our results can be explained as follows: a higher step frequency reduces the stimulation duration in each sequence, leading to smaller angular displacement of the leg and hence a shorter

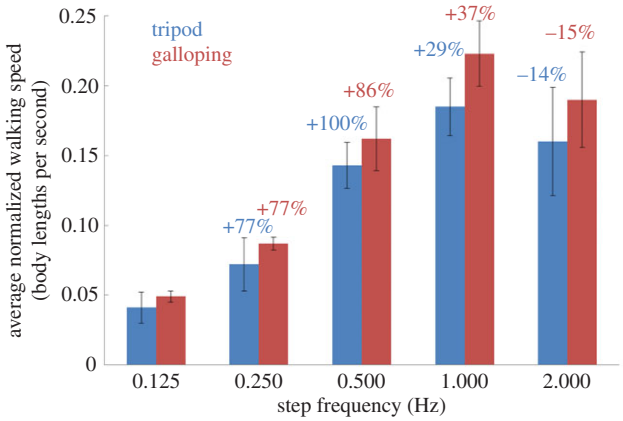

Figure 8. Average normalized walking speed (body lengths per second as a function of step frequency ($N = 6$ beetles, $n = 90$ data points). The walking speed study yielded 90 data points (nine data points per step frequency in each walking gait). Five continuous steps (the first and last steps were not counted) were used to obtain one average walking speed data point. The black bars indicate the standard deviations. For a given step frequency, the insect–computer hybrid robot progressed faster during galloping than during tripod walking. In both gaits, the average normalized walking speed increased with each doubling of the step frequency from 0.125 to 1 Hz, and then decreased from 1 to 2 Hz. The blue and red numbers indicate the percentage change of the average normalized walking speed at each doubling of the step frequency during tripod and galloping walking, respectively. See also the electronic supplementary material, movie S1.

step length. This phenomenon has been demonstrated in [6]. Therefore, we further investigated the robot's step length at different step frequencies (figure 9). In general, the robot's average normalized step length decreased with increasing step frequency (because the stimulation duration was shorter), except when the step frequency was doubled from 0.25 to 0.5 Hz. For instance, when the step frequency was doubled from 1 to 2 Hz, the average normalized step length was reduced by 55% and 53% during tripod and galloping walking, respectively (in other words, for both gaits, the average normalized step length at 2 Hz was less than half of that at

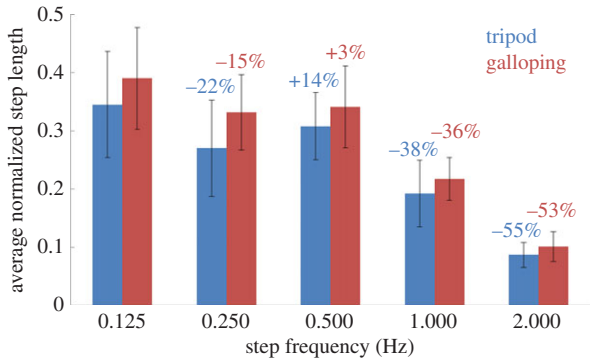

Figure 9. Average normalized step length versus step frequency ($N = 6$ beetles, $n = 150$ data points). Blue and red numbers indicate the percentage change of the average normalized step length at each doubling of the step frequency during tripod and galloping walking, respectively. In both gaits, the average normalized step length decreased with increasing step frequency, except for the doubling from 0.25 to 0.5 Hz. Note that the step length was measured as the linear distance between consecutive AEPs of the front legs. See also the electronic supplementary material, movie S1.

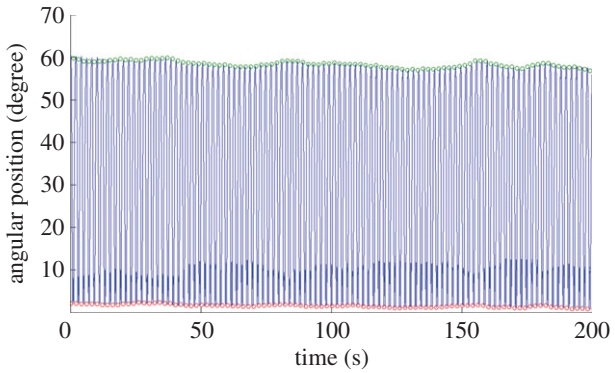

Figure 10. Repeatability test: cycles of leg motion induced by the electrical stimulation of the retraction and protraction muscles. A leg's motion (over a duration of 20 s) tracked in the repeatability test. Custom-developed MATLAB® code was used to automatically detect the angular positions of extreme retraction (green circles) and extreme protraction (red circles) with respect to the maximum protraction position reached during the 30 min stimulation (angular position = 0°). The beetle's leg keeps moving between the extreme retraction and protraction positions every second due to the applied electrical stimulation. The difference between adjacent retraction and protraction positions is the leg's angular displacement.

1 Hz). Therefore, doubling the step frequency from 1 to 2 Hz reduced the average normalized walking speed by 14% and 15% during tripod and galloping walking, respectively. In summary, changing the stimulation duration of each sequence affects both the step frequency and step length.

If the step frequency is further doubled from 2 to 4 Hz (corresponding to a stimulation duration of 62.5 ms in each sequence), the beetles could not progress in either gait, because the leg could not reach sufficient angular displacement for effective walking control within 62.5 ms. The angular displacement as a function of time in all six front leg motions (namely, protraction/retraction, levation/depression and extension/flexion) has been investigated at stimulation frequencies ranging from 10 to 100 Hz (in 10 Hz increments) and a stimulation amplitude of 1.5 V [6]. During protraction, levation and depression at 100 Hz, the leg approached its maximum angular displacement in 0.2–0.25 s. If the stimulation duration is very short (e.g. 62.5 ms at 4 Hz), the angular displacement of the leg is too small to initiate walking. When the leg could not be lifted from the ground during levation, it maintained contact with the ground at all times. Consequently, the beetle moved back and forth with its two front legs remaining at the same ground contact positions.

The range of step length of the insect–computer hybrid robot (min: 0.09 ± 0.02, max: 0.39 ± 0.09 body length as in figure 9) covers the voluntary walking's step length (0.24 ± 0.08 body length), which indicates that the insect–computer hybrid robot demonstrated the wider walking speed control and achieved both faster and slower walking than intact beetles. The average step frequency of the voluntary walking beetle is 1.66 ± 0.93 Hz, while the step frequency demonstrated in this study ranges from 0.125 to 2.00 Hz. Step frequency over 2.00 Hz was not usable because the stimulation duration is too short to induce sufficient contraction in the leg muscles. By increasing the stimulation frequency (which was set at constant in this study), the maximum step frequency for sufficient contraction can be increased [6], and, then, the walking speed is also increased. In fact, a cockroach increases the walking speed linearly with step frequency (constant step length). Once the step frequency reaches the maximum attainable value, the cockroach then increases the step length to further increase the walking speed [15]. The insect–computer hybrid robot has the same strategy (altering the step frequency and step length) to widely control the walking speed as both the step frequency and step length are user adjustable.

3.4. Repeatability of leg motions

Compared with man-made robots and actuators, when the same control input is applied repeatedly, the variances or errors in motor actions of electrically stimulated muscles (hence the induced appendage motion amplitude) is relatively large (figures 8–11) due to biological experimental factors such as individual animal difference and implanted electrode drift. However, the levels of variances and errors in muscle motor actions themselves are mostly less than 20% as in the standard deviations, which indicates the repeatability in the insect–computer hybrid robot. If the repeatability is low, there would be an increase, decrease, abrupt jump or cessation in motor action but, as shown in figure 10, the angular displacement (the length between the green and red plots) did not largely change throughout the trial. In addition, ANOVA test results showed that there was no clear day-by-day or animal-to-animal difference in the mean angular displacement ($F_{6,18} = 0.67$, $p = 0.67$ for test day effect; $F_{3,18} = 1.82$, $p = 0.18$ for beetle effect) or in the standard deviation ($F_{6,18} = 0.82$, $p = 0.57$ for test day effect; $F_{3,18} = 2.83$, $p = 0.07$ for beetle effect). The variation in the mean and standard deviation of the leg's angular displacement with respect to the individual beetle and test day is also shown in figure 11. We thus conclude that the insect–computer hybrid robot can repeatedly demonstrate desired and expected performances, i.e. the walking speed and step length are controllable by the step frequency as shown in figures 8 and 9. The relatively large variance (standard deviation of the order of 20%) does not strongly affect the walking performances. Such a large variance should be problematic in more sophisticated and precise locomotion control, for example regulating individual legs in pre-determined motion paths. In that case, closed-loop (feedback) control coupled with leg motion detection should be adopted for the insect–computer hybrid robot [6].

Also the small fluctuation in the variance level implies that the animal's voluntary motor action did not significantly

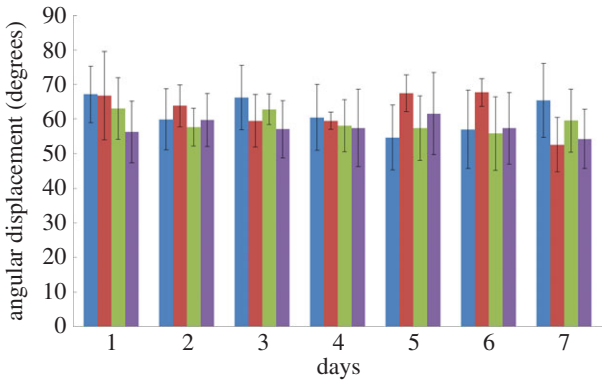

Figure 11. Repeatability test: the average and standard deviation of four beetles' front leg angular displacement ($N = 4$ beetles, $n = 1800$ data points). Every beetle was stimulated for more than 30 min per day for 7 consecutive days. The four different colours of the columns indicate the four tested beetles. The standard deviations are indicated by the black bars. The mean and standard deviation of the leg's angular displacement of each beetle on each day were calculated from more than 1800 data points (refer to figure 10 for the data points allocation method), which resulted from the more than 30 min stimulation (as the protraction and retraction muscles of the beetles were stimulated alternatively for 1 s).

affect the motor action induced by the electrical stimulations. If the animal voluntarily disturbed the electrically induced motor action and it strongly influenced the resultant displacement, the angular displacement shown in figure 10 would be abruptly changed, but such a large change was not seen in the data.

5. Conclusion

We demonstrated that *M. torquata* beetles can be controlled to walk in tripod and galloping gaits with predefined stimulation sequences (table 1). By altering the step frequency, we adjusted the step length and walking speed of the beetles. To the best of our knowledge, this is the first demonstration of living insect locomotion control with user-adjustable walking gaits, step lengths and walking speeds. With the 100% success rate of leg motion elicitation, the insect–computer hybrid robot demonstrated here is more reliable than those controlled by stimulation of neurons where habituation exists (e.g. antenna or ganglia). Moreover, compared with existing insect–computer hybrid robots in which the control of walking speed and gait is impossible, the ability to monitor the robot's walking speed and walking gait would enable it to complete more complicated tasks. Such regulation of the beetle's leg motions at predefined sequences and durations should significantly contribute to the future development of animal–computer hybrid robots. For instance, we could control the middle and hind legs of the beetle or regulate the appendage motions of other animals such as cockroaches and dragonflies for legged robots and unmanned aerial micro-vehicles. Furthermore, the stimulation protocol demonstrated can benefit biological research in the field such as testing the physical limit of muscles, comparing the energy efficiency of different walking gaits and confirming the hypothetical functions of muscles.

Authors' contributions. F.C. and H.S. conceived and designed the experiments. F.C., C.Z., H.Y.C. and H.S. performed the experiments. F.C., H.Y.C. and H.S. analysed the data. F.C. and H.S. wrote the manuscript. All authors reviewed the manuscript.

Competing interests. The authors have declared that no competing interests exist.

Funding. The work is financially supported by Agency for Science, Technology and Research (A*STAR) Public Sector Research Funding (PSF, M4070190), a Nanyang Assistant Professorship (NAP, M4080740) and an A*STAR-JST (The Japan Science and Technology Agency) joint grant, M4070198.

Acknowledgement. The authors offer their appreciation to Mr Tat Thang Vo Doan, Mr Yao Li, Mr Chew Hock See and Mr Roger Tan Kay Chia at the School of Mechanical and Aerospace Engineering, Nanyang Technological University.

References

1. Abbott A. 2007 Biological robotics: working out the bugs. *Nature* **445**, 250–253. (doi:10.1038/445250a)
2. Krieger MJ, Billeter J-B, Keller L. 2000 Ant-like task allocation and recruitment in cooperative robots. *Nature* **406**, 992–995. (doi:10.1038/35023164)
3. Wootton R. 2000 Aerodynamics: from insects to microvehicles. *Nature* **403**, 144–145. (doi:10.1038/35003074)
4. Ma KY, Chirarattananon P, Fuller SB, Wood RJ. 2013 Controlled flight of a biologically inspired, insect-scale robot. *Science* **340**, 603–607. (doi:10.1126/science.1231806)
5. Koh J-S *et al.* 2015 Jumping on water: surface tension-dominated jumping of water striders and robotic insects. *Science* **349**, 517–521. (doi:10.1126/science.aab1637)
6. Cao F *et al.* 2014 A biological micro actuator: graded and closed-loop control of insect leg motion by electrical stimulation of muscles. *PLoS ONE* **9**, e105389. (doi:10.1371/journal.pone.0105389)
7. Sato H, Berry CW, Peeri Y, Baghoomian E, Casey BE, Lavella G, VandenBrooks JM, Harrison J, Maharbiz MM. 2010 Remote radio control of insect flight. *Front. Integr. Neurosci.* **3**, 24.
8. Kohut NJ, Birkmeyer PM, Peterson KC, Fearing RS. 2012 Maneuverability and mobility in palm-sized legged robots. In *Micro- and nanotechnology sensors, systems, and applications IV* (eds T George, MS Islam, A Dutta), pp. 837 311–837 319. Bellingham, WA: Spie-Int Soc Optical Engineering.
9. Shoji K, Akiyama Y, Suzuki M, Hoshino T, Nakamura N, Ohno H, Morishima K. 2012 Insect-mountable biofuel cell with self-circulation system. In *Proc. of the 2012 IEEE 25th Int. Conf. on Micro Electro Mechanical Systems (MEMS), Paris, France, 29 January–2 February 2012*, pp. 1249–1252. Piscataway, NJ: IEEE.
10. Reissman T, MacCurdy RB, Garcia E. 2011 Electrical power generation from insect flight. *Proc. Soc. Photo-opt. Instrument. Eng.* **7977**, 797 702–797 709. (doi:10.1117/12.880702)
11. Shoji K, Akiyama Y, Suzuki M, Hoshino T, Nakamura N, Ohno H, Morishima K. 2012 Insect biofuel cells using trehalose included in insect hemolymph leading to an insect-mountable biofuel cell. *Biomed. Microdevices* **14**, 1063–1068. (doi:10.1007/s10544-012-9706-z)
12. Halamkova L, Halamek J, Bocharova V, Szczupak A, Alfonta L, Katz E. 2012 Implanted biofuel cell operating in a living snail. *J. Am. Chem. Soc.* **134**, 5040–5043. (doi:10.1021/ja211714w)
13. Shoji K, Akiyama Y, Suzuki M, Nakamura N, Ohno H, Morishima K. 2013 Gold nanoparticle-based biofuel cell using insect body fluid circulation. In *Proc. 2013 Transducers & Eurosensors XXVII: The 17th Int. Conf. on Solid-State Sensors, Actuators and Microsystems (TRANSDUCERS & EUROSENSORS XXVII), Barcelona, Spain, 13–June 2013*, pp. 2811–2814 Piscataway, NJ: IEEE.
14. Shoji K, Akiyama Y, Suzuki M, Nakamura N, Ohno H, Morishima K. 2014 Diffusion refueling biofuel cell

mountable on insect. In *Proc. 2014 IEEE 27th Int. Conf. on Micro Electro Mechanical Systems* (*MEMS*), *San Francisco, CA, 26–30 January 2014*, pp. 163–166. Piscataway, NJ: IEEE.

15. Full RJ, Tu MS. 1990 Mechanics of 6-legged runners. *J. Exp. Biol.* **148**, 129–146.
16. Dickinson MH, Farley CT, Full RJ, Koehl MAR, Kram R, Lehman S. 2000 How animals move: an integrative view. *Science* **288**, 100–106. (doi:10.1126/science.288.5463.100)
17. Full RJ, Tu MS. 1991 Mechanics of a rapid running insect—2-legged, 4-legged and 6-legged locomotion. *J. Exp. Biol.* **156**, 215–231.
18. Full RJ, Stokes DR, Ahn AN, Josephson RK. 1998 Energy absorption during running by leg muscles in a cockroach. *J. Exp. Biol.* **201**, 997–1012.
19. Full RJ, Kubow T, Schmitt J, Holmes P, Koditschek D. 2002 Quantifying dynamic stability and maneuverability in legged locomotion. *Integr. Comp. Biol.* **42**, 149–157. (doi:10.1093/icb/42.1.149)
20. Sato H *et al.* 2015 Deciphering the role of a coleopteran steering muscle via free flight stimulation. *Curr. Biol.* **25**, 798–803. (doi:10.1016/j.cub.2015.01.051)
21. Daly DC, Mercier PP, Bhardwaj M, Stone AL, Aldworth ZN, Daniel TL, Voldman J, Hildebrand JG, Chandrakasan AP. 2010 A pulsed UWB receiver SoC for insect motion control. *IEEE J. Solid-State Circuits* **45**, 153–166. (doi:10.1109/jssc.2009.2034433)
22. Wang HZ, Ando NY, Kanzaki RH. 2008 Active control of free flight manoeuvres in a hawkmoth, *Agrius convolvuli*. *J. Exp. Biol.* **211**, 423–432. (doi:10.1242/jeb.011791)
23. Tubbs TB, Palazotto AN, Willis MA. 2011 Biological investigation of wing motion of the *Manduca sexta*. *Int. J. Micro Air Vehicles* **3**, 101–117. (doi:10.1260/1756-8293.3.2.101)
24. Bozkurt A, Gilmour RF, Lal A. 2009 Balloon-assisted flight of radio-controlled insect biobots. *IEEE Trans. Biomed. Eng.* **56**, 2304–2307. (doi:10.1109/tbme.2009.2022551)
25. Tsang WM, Stone AL, Aldworth ZN, Hildebrand JG, Daniel TL, Akinwande AI, Voldman J. 2010 Flexible split-ring electrode for insect flight biasing using multisite neural stimulation. *IEEE Trans. Biomed. Eng.* **57**, 1757–1764. (doi:10.1109/tbme.2010.2041778)
26. Bozkurt A, Gilmour RF, Sinha A, Stern D, Lal A. 2009 Insect-machine interface based neurocybernetics. *IEEE Trans. Biomed. Eng.* **56**, 1727–1733. (doi:10.1109/tbme.2009.2015460)
27. Bozkurt A, Gilmour R, Stern D, Lal A. 2008 MEMS based bioelectronic neuromuscular interfaces for insect cyborg flight control. In *Mems 2008: 21st IEEE Int. Conf. on Micro Electro Mechanical Systems, Technical Digest*, pp. 160–163. New York, NY: IEEE.
28. Hinterwirth AJ, Medina B, Lockey J, Otten D, Voldman J, Lang JH, Hildebrand JG, Daniel TL. 2012 Wireless stimulation of antennal muscles in freely flying hawkmoths leads to flight path changes. *PLoS ONE* **7**, e52725. (doi:10.1371/journal.pone.0052725)
29. Latif T, Bozkurt A. 2012 Line following terrestrial insect biobots. In *Proc. 2012 34th Annu. Int. Conf. of the IEEE Engineering in Medicine and Biology Society* (*EMBC*), *San Diego, CA, 28 August–1 September 2012*, pp. 972–975. Piscataway, NJ: IEEE.
30. Latif T, Whitmire E, Novak T, Bozkurt A. 2015 Sound localization sensors for search and rescue biobots. *Sensors J. IEEE*. **PP**, 1–1. (doi:10.1109/JSEN.2015.2477443)
31. Sanchez CJ, Chiu C-W, Zhou Y, Gonzalez JM, Vinson SB, Liang H. 2015 Locomotion control of hybrid cockroach robots. *J. R. Soc. Interface* **12**, 20141363. (doi:10.1098/rsif.2014.1363)
32. Erickson JC, Herrera M, Bustamante M, Shingiro A, Bowen T. 2015 Effective stimulus parameters for directed locomotion in Madagascar hissing cockroach biobot. *PLoS ONE* **10**, e0134348. (doi:10.1371/journal.pone.0134348)
33. Giampalmo SL, Absher BF, Bourne WT, Steves LE, Vodenski VV, O'Donnell PM, Erickson JC. 2011 Generation of complex motor patterns in American grasshopper via current-controlled thoracic electrical interfacing. In *Proc. 2011 33rd Annu. Int. Conf. of the IEEE Engineering in Medicine and Biology Society* (*EMBC*), *Boston, MA, 30 August–3 September 2011*, pp. 1275–1278. Piscataway, NJ: IEEE.
34. Chuan Z, Jingquan L, Hongchang T, Xiaoyang K, Yuefeng R, Bin Y, Hongying Z, Chunsheng Y. 2013 Control of swimming in crucian carp: stimulation of the brain using an implantable wire electrode. In *Proc. 2013 8th IEEE Int. Conf. on Nano/Micro Engineered and Molecular Systems* (*NEMS*), *Suzhou, China, 7–10 April 2013*, pp. 360–363. Piscataway, NJ: IEEE.
35. Zhang C, Liu J-Q, Tian H-C, Kang X-Y, Du J-C, Rui Y-F, Yang B, Yang C-S. 2015 Implantable electrode array with platinum black coating for brain stimulation in fish. *Microsyst. Technol.* **21**, 139–145. (doi:10.1007/s00542-013-2017-3)
36. Chung AJ, Cordovez B, Jasuja N, Lee DJ, Huang XT, Erickson D. 2012 Implantable microfluidic and electronic systems for insect flight manipulation. *Microfluid. Nanofluid.* **13**, 345–352. (doi:10.1007/s10404-012-0957-z)
37. Tsang WM, Stone A, Aldworth Z, Otten D, Akinwande AI, Daniel T, Hildebrand JG, Levine RB, Voldman J. 2010 Remote control of a cyborg moth using carbon nanotube-enhanced flexible neuroprosthetic probe. In *Proc. 2010 IEEE 23rd Int. Conf. on Micro Electro Mechanical Systems* (*MEMS*), *Wanchai, Hong Kong, 24–28 January 2010*, pp. 39–42. Piscataway, NJ: IEEE.
38. Mann K, Massey TL, Guha S, van Kleef JP, Maharbiz MM. 2014 A wearable wireless platform for visually stimulating small flying insects. In *Proc. 2014 36th Annu. Int. Conf. of the IEEE Engineering in Medicine and Biology Society* (*EMBC*), *Chicago, IL, 26–30 August 2014*, pp. 1654–1657. Piscataway, NJ: IEEE.
39. Li B, Nenggan Z, Huixia Z, Yaoyao H, Huoqing Z, Fuliang H, Xiaoxiang Z. 2011 Flight control of tethered honeybees using neural electrical stimulation. In *Proc. 2011 5th Int. IEEE/EMBS Conf. on Neural Engineering* (*NER*), *Cancun, Mexico, 27 April–1 May 2011*, pp. 558–561. Piscataway, NJ: IEEE.
40. Zhao H, Zheng N, Ribi WA, Zheng H, Xue L, Gong F, Zheng X, Hu F. 2014 Neuromechanism study of insect–machine interface: flight control by neural electrical stimulation. *PLoS ONE* **9**, e113012. (doi:10.1371/journal.pone.0113012)
41. Whitmire E, Latif T, Bozkurt A. 2013 Kinect-based system for automated control of terrestrial insect biobots. In *Proc. 2013 35th Annu. Int. Conf. of the IEEE Engineering in Medicine and Biology Society* (*EMBC*), *Osaka, Japan, 3–7 July 2013*, pp. 1470–1473. Piscataway, NJ: IEEE.
42. Holzer R, Shimoyama I. 1997 Locomotion control of a bio-robotic system via electric stimulation. In *Proc. of the 1997 IEEE/RSJ Int. Conf. on Intelligent Robot and Systems. Innovative Robotics for Real-World Applications. IROS '97, Grenoble, France, 7–11 September 1997*, pp. 1514–1519. Piscataway, NJ: IEEE.
43. Bozkurt A *et al.* 2014 Biobotic insect swarm based sensor networks for search and rescue. *Signal Process. Sensor/Inform. Fusion Target Recogn. Xxiii* **9091**, 90911 L. (doi:10.1117/12.2053906)
44. Moore TE, Crary SB, Koditschek DE, Conklin TA. 1998 Directed locomotion in cockroaches: biobots. *Acta Entomol. Sloven.* **6**, 71–78.
45. Lemmerhirt DR, Staudacher EM, Wise KD. 2006 A multitransducer microsystem for insect monitoring and control. *IEEE Trans. Biomed. Eng.* **53**, 2084–2091. (doi:10.1109/tbme.2006.877115).
46. Yang ZL, Chun KY, Xu JY, Lin F, Li DQ, Ren HL. 2014 A preliminary study of motion control patterns for biorobotic spiders. In *Proc. 2014 11th IEEE Int. Conf. on Control & Automation* (*ICCA*), *Taichung, Taiwan, 18–20 June 2014*, pp. 128–132. Piscataway, NJ: IEEE.
47. Wilson DM. 1966 Insect walking. *Annu. Rev. Entomol.* **11**, 103–122. (doi:10.1146/annurev.en.11.010166.000535).
48. Smolka J, Byrne MJ, Scholtz CH, Dacke M. 2013 A new galloping gait in an insect. *Curr. Biol.* **23**, R913–R915. (doi:10.1016/j.cub.2013.09.031)
49. Jamon M, Clarac F. 1995 Locomotor patterns in freely moving crayfish (*Procambarus clarkii*). *J. Exp. Biol.* **198**, 683–700.
50. Fischer H, Schmidt J, Haas R, Buschges A. 2001 Pattern generation for walking and searching movements of a stick insect leg. I. Coordination of motor activity. *J. Neurophysiol.* **85**, 341–353.
51. Chasserat C, Clarac F. 1986 Basic processes of locomotor coordination in the rock lobster. 2. Simulation of leg coupling. *Biol. Cybern.* **55**, 171–185.
52. Haldane DW, Peterson KC, Bermudez FLG, Fearing RS. 2013 Animal-inspired design and aerodynamic stabilization of a hexapedal millirobot. In *Proc. ICRA 2013—IEEE Int. Conf. on Robotics and Automation, Karlsruhe, Germany, 6–10 May 2013*, pp. 3279–3286. Piscataway, NJ: IEEE.